

Excitonic enhancement of nonradiative energy transfer from a quantum well in the optical near field of energy gradient quantum dots

Sedat Nizamoglu, Pedro Ludwig Hernández-Martínez, Evren Mutlugun, Durmus Ugur Karatay, and Hilmi Volkan Demir

Citation: *Appl. Phys. Lett.* **100**, 241109 (2012); doi: 10.1063/1.4724109

View online: <http://dx.doi.org/10.1063/1.4724109>

View Table of Contents: <http://apl.aip.org/resource/1/APPLAB/v100/i24>

Published by the American Institute of Physics.

Related Articles

Role of heteroepitaxial misfit strains on the band offsets of Zn_{1-x}BexO/ZnO quantum wells: A first-principles analysis

J. Appl. Phys. **111**, 113714 (2012)

Transport of indirect excitons in a potential energy gradient

Appl. Phys. Lett. **100**, 231106 (2012)

ZnO/(ZnMg)O single quantum wells with high Mg content graded barriers

J. Appl. Phys. **111**, 113504 (2012)

A simple analysis of interband absorption in quantum well structure of III-V ternary and quaternary semiconductors

J. Appl. Phys. **111**, 103104 (2012)

Two-dimensional electron gas mobility limited by barrier and quantum well thickness fluctuations scattering in Al_xGa_{1-x}N/GaN multi-quantum wells

Appl. Phys. Lett. **100**, 162102 (2012)

Additional information on *Appl. Phys. Lett.*

Journal Homepage: <http://apl.aip.org/>

Journal Information: http://apl.aip.org/about/about_the_journal

Top downloads: http://apl.aip.org/features/most_downloaded

Information for Authors: <http://apl.aip.org/authors>

ADVERTISEMENT



Agilent Technologies

Agilent Education and Research Resources DVD 2012

Packed with over **100 NEW** articles, application notes, webcasts, and videos relating to Renewable Energy, Nanoscience, RF/Wireless, MIMO, Materials, Digital Signals, Photonics, and General Test & Measurement.

Click Here to
Order Your DVD



Agilent Technologies

Excitonic enhancement of nonradiative energy transfer from a quantum well in the optical near field of energy gradient quantum dots

Sedat Nizamoglu,^{1,a)} Pedro Ludwig Hernández-Martínez,^{1,2} Evren Mutlugun,^{1,2} Durmus Ugur Karatay,¹ and Hilmi Volkan Demir^{1,2,b)}

¹Department of Electrical and Electronics Engineering, Department of Physics, UNAM—National Nanotechnology Research Center, and Institute of Materials Science and Nanotechnology, Bilkent University, Ankara TR-06800, Turkey

²Luminous! Center of Excellence for Semiconductor Lighting and Displays, School of Electrical and Electronic Engineering, School of Physical and Mathematical Sciences, Nanyang Technological University, Singapore 639798, Singapore

(Received 29 March 2012; accepted 30 April 2012; published online 13 June 2012)

We report strong exciton migration with an efficiency of 83.3% from a violet-emitting epitaxial quantum well (QW) to an energy gradient colloidal construct of layered green- and red-emitting nanocrystal quantum dots (NQDs) at room temperature, enabled by the interplay between the exciton population and the depopulation of states in the optical near field. Based on the density matrix formalization of near-field interactions, we theoretically model and demonstrate that the energy gradient significantly boosts the QW-NQDs exciton transfer rate compared to using mono-dispersed NQDs, which is in agreement with the observed experimental results. © 2012 American Institute of Physics. [<http://dx.doi.org/10.1063/1.4724109>]

Efficient exciton transfer from epitaxial quantum wells (QWs) to colloidal nanocrystal quantum dots (NQDs) is critical to the energy efficiency in hybrid optoelectronic devices in which QWs and NQDs are interfaced, including color conversion light emitting diodes (LEDs) of NQD nanophosphors. Previously, Basko *et al.* theoretically proposed that Förster-type nonradiative energy transfer (ET) can be used as an efficient means of pumping luminescent materials,¹ and Achermann *et al.* experimentally demonstrated ET pumping of semiconductor nanocrystals using an epitaxial quantum well² in a LED architecture.³ Additionally, white light generating ET pumping was also later shown.⁴ However, for a practical implementation of ET pumping in a standard electrically driven LED device, there exist two competing factors. One is that a relatively thicker contact layer is needed for efficient current injection into the quantum well region to avoid current crowding. The other is that the distance (d) dependence of the energy transfer rate ($\propto d^{-4}$) in the planar configuration, which forces to use exceedingly thin layers. By considering this trade-off, Achermann *et al.* integrated CdSe nanocrystal quantum dots on top of a very thin capping layer of 3 nm in thickness.³ Although the energy transfer was achieved, the resulting energy transfer efficiency was yet less than 50% at room temperature. Also, previously multiple layers of NQDs were investigated for excitonic energy transfer among the NQDs.^{5,6} Enhanced photoluminescence was observed in these NQD systems, which was attributed to the recycling of trapped excitons via Förster-type nonradiative energy transfer. Such layered NQDs were also used to tune the color by ET within the NQDs.⁷

Different than the prior reports, we propose and demonstrate enhanced nonradiative energy transfer from a quantum

well to an energy gradient structure consisting of NQD bilayer, as opposed to mono-dispersed NQDs. We report strong exciton migration with a substantially improved transfer efficiency of 83.3% at room temperature for the cascaded QW-NQDs construct with a top-capping layer (~ 3 nm) as sketched in the inset of Fig. 1. Using green- and red-emitting NQD bilayer on the violet-emitting quantum well with the top GaN capping layer, the energy gradient layer increases the exciton transfer efficiency by 64.2% with respect to the bilayer of mono-dispersed red-emitting NQDs. Through modeling this energy transfer cascade based on the optical near field approach, this excitonic enhancement of nonradiative energy transfer can be explained by the exciton population and depopulation dynamics of the NQDs.

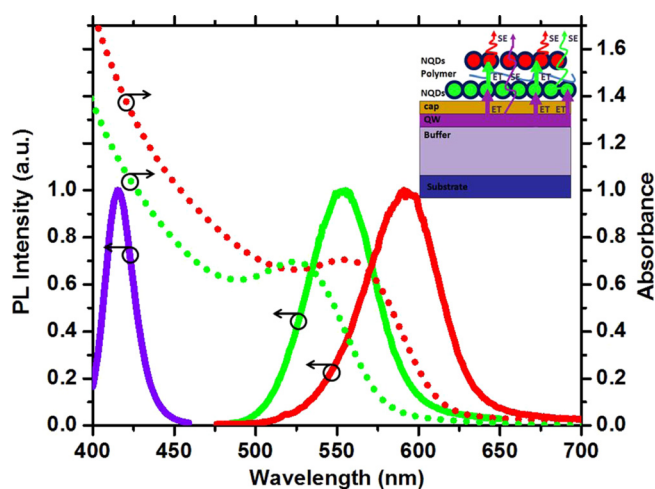


FIG. 1. Emission spectra of InGaN/GaN quantum well (violet solid line) and CdTe nanocrystal quantum dots (green and red solid lines for green- and red-emitting NQDs, respectively), and absorption spectra of CdTe nanocrystal quantum dots (green and red dotted lines for green and red-emitting NQDs, respectively). A schematic representing the hybrid structure of CdTe NQDs bilayer integrated on the InGaN/GaN quantum well is shown. (ET and SE represent exciton transfer and spontaneous emission, respectively.)

^{a)}Present address: Wellman Center, Harvard Medical School, 65 Landsdowne Street, Cambridge, Massachusetts 02139, USA.

^{b)}Email: volkan@stanfordalumni.org.

For our QW-NQD hybrid model system, we grew a single InGaN/GaN QW emitting in violet region using standard metal organic chemical vapor deposition. For the nanophosphors, we synthesized thiol-capped green- and red-emitting CdTe NQDs following standard colloidal synthesis.⁸ The emission spectra of the resulting QW and NQDs are shown in Fig. 1. To form the QW-NQD hybrid system, we assembled NQDs layer by layer. We prepared samples consisting of bilayers of only green-emitting NQDs, of only red-emitting NQDs, and of green- and red-emitting NQDs. For time-resolved spectroscopy, we employed a FluoTime 200 spectrometer (from PicoQuant) with a calibrated time resolution of 32 ps, along with a pulsed laser diode at 375 nm as the excitation signal and a photon multiplier tube as the detector. We measured the time-resolved dynamics of the hybrid system at 414, 530, and 610 nm, which correspond to the respective emission peaks of the violet-emitting QW and the green- and red-emitting NQDs. Because of the finite temporal response of the pulsed laser excitation as shown in Fig. 2, the decay dynamics measured in experiments include the photoluminescence decay convoluted with the laser response. For the data analysis, we utilized FluoFit software by means of which we introduced the instrumental response function in our analysis. Using the numerical fitting module of FluoFit, due to the convolution, the resulting numerical fits were not pure exponential functions, similar to the measured time-resolved responses.

We investigated the QW emission dynamics at the wavelength of 414 nm as the exciton donor for the integrated NQD bilayer. As the reference, the lifetime of the quantum well alone (without NQDs) is measured to be 1.32 ns (i.e., $\gamma_{QW} = 0.757 \text{ ns}^{-1}$). After the integration of the energy gradient bilayer consisting of green- and red-emitting CdTe NQDs on the QW, the lifetime is shortened down to 0.22 ns (i.e., $\gamma_{HYBRID} = 4.545 \text{ ns}^{-1}$). By subtracting the rate of the hybrid structure from the only QW case (i.e., $\gamma_{ET} = \gamma_{QW} - \gamma_{HYBRID}$), we predict an exciton transfer rate of $\gamma_{ET} = 3.787 \text{ ns}^{-1}$. We calculate the exciton transfer efficiency using $\eta = \gamma_{ET} / (\gamma_{ET} + \gamma_{QW})$ and the resulting ET efficiency is found to be 83.3%. This strong ET efficiency means that most of the generated excitons in the QW are transferred to the NQDs. To

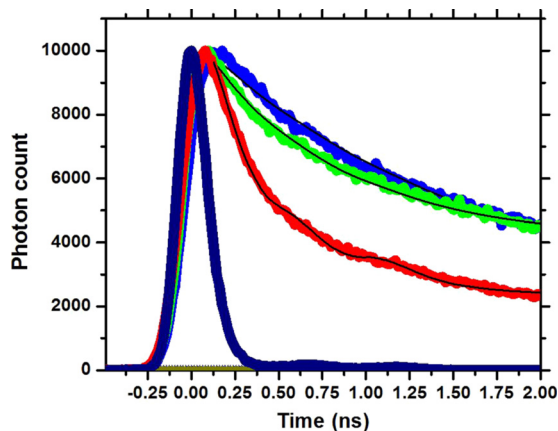


FIG. 2. Time-resolved spectroscopy at 414 nm of only quantum well (in blue color), green- and red-emitting CdTe NQDs bilayer integrated on the InGaN/GaN quantum well (in red color), red- and red-emitting CdTe NQDs bilayer integrated on the InGaN/GaN quantum well (in green color), and laser diode response function (in navy color).

observe the effect of the energy gradient, we also studied the case for a bilayer of only red-emitting NQDs. In this configuration, the QW lifetime at 414 nm is found to be longer than that in the hybrid case of green- and red-emitting NQDs integrated on the QW because the bilayer of red-emitting NQDs does not form a strong internal energy gradient for excitons in QW to be efficiently advanced toward the last NQD layer. Fig. 2 shows that the QW photoluminescence decay using the red-emitting NQD bilayer is slower with respect to that using the energy gradient construct. The QW lifetime in the presence of the red-emitting NQDs bilayer is measured to be 0.65 ns. Thus, in the case of using the red-emitting NQD bilayer, the exciton transfer is observed to be weaker, with a lower rate of 0.780 ns^{-1} and a smaller ET efficiency level of 50.7%. Therefore, for efficient exciton migration from QW to NQDs, the hybridization of energy gradient is more advantageous.

We further investigated the exciton transfer dynamics at the acceptor green- and red-emitting NQD emission peaks to verify that the decreased lifetime of the donors results from the Förster-type exciton transfer to the acceptors. The exciton dynamics for the green-emitting NQDs at 530 nm is provided in the inset of Fig. 3. We observe an increased green NQD lifetime for the hybrid green- and red-emitting NQD bilayers on the QW because of strong energy feeding from the QW with respect to the control groups of only green-emitting NQDs bilayer on glass substrate, and green- and red-emitting NQDs bilayers on the glass substrate. In Fig. 3, the time-resolved spectroscopy for the red-emitting NQDs at 610 nm is shown. Here, the red NQD decay of the green- and red-emitting NQD bilayers on the QW is significantly slower than the control groups. Furthermore, the decay of the energy gradient bilayer reaches its maximum later than the other control groups again because of the strong exciton feeding. As a result, we can conclusively state that excitons are transferred from the QWs to the NQDs via Förster-type

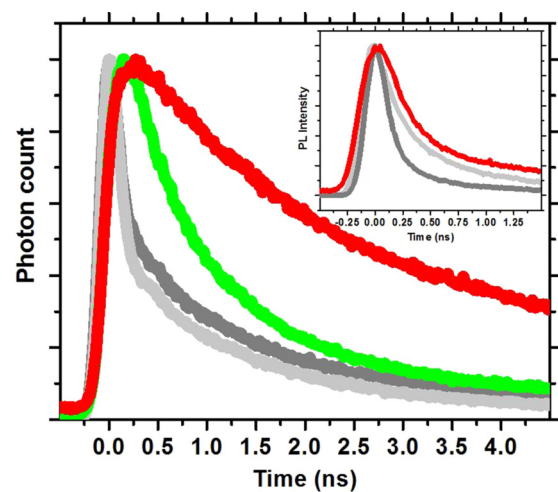


FIG. 3. Time-resolved spectroscopy at 610 nm of green- and red-emitting CdTe NQDs bilayer integrated on the InGaN/GaN quantum well (in red color), red- and red-emitting CdTe NQDs bilayer integrated on the InGaN/GaN quantum well (in green color), green- and red-emitting CdTe NQDs bilayer integrated on glass substrate (in dark grey color), and red- and red-emitting CdTe NQDs bilayer integrated on glass substrate (in light grey color). Inset shows the time-resolved spectroscopy at the emission wavelength of 530 nm.

nonradiative energy transfer and substantially more in the case of energy gradient NQD bilayer.

We also theoretically investigate exciton transfer in the QW/NQD/NQD hybrid system by developing a model based on density matrix formalization of near-field interactions (see supplementary material¹⁰). We first consider the excitation transfer between a QW to a bilayer of the green- and red-emitting NQDs. The energy diagram for this configuration is given in the inset of Fig. 4. The density matrix ρ^{AB} , which corresponds to the energy level E_1 , is governed by the master equation

$$\frac{\partial \rho^{AB}}{\partial t} = -\frac{i}{\hbar} [V_{NF,AB}, \rho^{AB}] - (N_{\Gamma}^{AB} \rho^{AB} + \rho^{AB} N_{\Gamma}^{AB}), \quad (1)$$

where N_{Γ}^{AB} is a diagonal matrix whose diagonal elements are given by γ_{α} and Γ_{α} . Here, γ_{α} is the exciton recombination rate ($\gamma_{\alpha} = 1/\tau_{\alpha}$) and Γ_{α} is the sublevel relaxation rate. $V_{NF,AB}$ is the interaction between the levels with energy E_1 given by $\hbar U_{AB}$. The master equation corresponding to the density matrix ρ^{BC} with the energy level E_2 can be written as

$$\frac{\partial \rho^{BC}}{\partial t} = -\frac{i}{\hbar} [V_{NF,BC}, \rho^{BC}] - (N_{\Gamma}^{BC} \rho^{BC} + \rho^{BC} N_{\Gamma}^{BC}) + P_{\Gamma}[\rho^{AB}], \quad (2)$$

where $P_{\Gamma}(\rho^{AB})$ represents the relaxation from the energy level E_1 to E_2 ; $V_{NF,BC}$ and N_{Γ}^{BC} are defined similar to Eq. (1). Finally, the master equation for the density matrix ρ^C with the energy level E_3 is derived as

$$\frac{\partial \rho^C}{\partial t} = -(N_{\Gamma}^C \rho^C + \rho^C N_{\Gamma}^C) + P_{\Gamma}[\rho^{BC}], \quad (3)$$

where $P_{\Gamma}(\rho^{BC})$ represents the relaxation from the energy level E_2 to E_3 , and N_{Γ}^C is a diagonal matrix with matrix elements γ_{α} . For the NQDs, we assume $\gamma_{QD1} \approx \gamma_{QD2} \approx \frac{1}{5 \text{ ns}}$ and $\Gamma_{QD1} \approx \Gamma_{QD2} \approx \frac{1}{10 \text{ ps}}$. For the QW, we take $\gamma_{QW} \approx \frac{1}{1.32 \text{ ns}}$. For

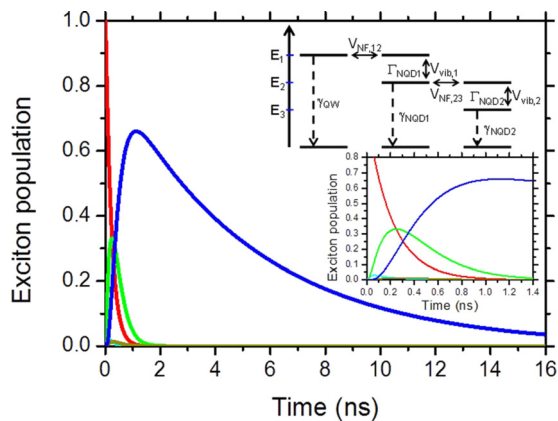


FIG. 4. Calculated exciton populations. Red line shows the exciton population of the first excited state in the QW. Cyan line depicts the exciton population of the second excited state for the green NQD layer. Green line shows the exciton population of the first excited state of the green NQD layer. Dark yellow line depicts the exciton population of the second excited state of the red NQD layer. Blue line illustrates the exciton population of the first excited state of the red NQD layer. Inset: Energy diagram for the QW, the first NQD layer and the second NQD layer.

the interaction between the nanocrystals, we use $U_{AB} = U_{BC} = \frac{1}{100 \text{ ps}}$.⁹ Next, we calculate the exciton population for each complex. We use the following matrices:

$$\begin{aligned} \rho^{AB} &= \begin{pmatrix} \rho_{11}^{AB} & \rho_{12}^{AB} \\ \rho_{21}^{AB} & \rho_{22}^{AB} \end{pmatrix}, \quad \rho^{BC} = \begin{pmatrix} \rho_{11}^{BC} & \rho_{12}^{BC} \\ \rho_{21}^{BC} & \rho_{22}^{BC} \end{pmatrix}, \quad \rho^C = \begin{pmatrix} \rho^C & 0 \\ 0 & 0 \end{pmatrix}, \\ V_{NF,AB} &= \begin{pmatrix} 0 & \hbar U_{AB} \\ \hbar U_{AB} & 0 \end{pmatrix}, \quad V_{NF,BC} = \begin{pmatrix} 0 & \hbar U_{BC} \\ \hbar U_{BC} & 0 \end{pmatrix}, \\ N_{\Gamma}^C &= \frac{1}{2} \begin{pmatrix} \gamma_{NQD2} & 0 \\ 0 & 0 \end{pmatrix}, \quad N_{\Gamma}^{AB} = \frac{1}{2} \begin{pmatrix} \gamma_{NQW} & 0 \\ 0 & \Gamma_{NQD1} \end{pmatrix}, \\ N_{\Gamma}^{BC} &= \frac{1}{2} \begin{pmatrix} \gamma_{NQD1} & 0 \\ 0 & \gamma_{NQD2} \end{pmatrix}, \quad P(\rho^{AB}) = \begin{pmatrix} \Gamma_{NQD1} \rho_{22}^{AB} & 0 \\ 0 & 0 \end{pmatrix}, \\ P(\rho^{BC}) &= \begin{pmatrix} \Gamma_{NQD2} \rho_{22}^{BC} & 0 \\ 0 & 0 \end{pmatrix}, \end{aligned} \quad (4)$$

where ρ^C is the exciton population of the first excited state of the second NQD layer, ρ_{11}^{AB} represents the exciton population of the first excited state in the QW, ρ_{22}^{AB} is the exciton population of the second excited state of the first NQD layer, ρ_{11}^{BC} gives the exciton population of the first excited state in the first NQD layer, and ρ_{22}^{BC} is the exciton population of the first excited state of the second NQD layer.

Numerical results for the exciton population are shown in Fig. 4. From this plot, it is observed that it takes about 1 ns for an exciton in the QW to be transferred to the second NQD layer. Also, this plot illustrates the exciton population of the intermediate states. The transfer efficiency from the QW to the last layer is about 70%, as depicted in Fig. 4. This result agrees with the experimental value of 83.3%. The advantage of the energy gradient NQDs system is that the exciton is funneling to the lowest energy state via near field interaction. This process is unidirectional because of the fast interband relaxation between the energy levels avoiding the nutation process between the dots. Therefore, the probability of exciton transfer to the first excited state of the second NQD layer from the other layer can significantly be improved. In the other case of exciton transfer from a QW to a bilayer of red-emitting NQDs, the nutation process between the first and second NQD layers is observed, meaning that the excitons oscillate between the first excited state of the NQDs (see supplementary material¹⁰). This is because of the fact that both layers are made of the same NQDs, and their energy levels are in resonance. The transfer efficiency from the QW to the last layer is about 45%, and this result also agrees with the experimental value of 50.7%. In summary, these results suggest that introducing an energy difference across the NQD layers in the optical near field enhances the exciton transfer from the QW to the last NQD layer.

In conclusion, we demonstrated strong exciton migration from an epitaxial quantum well to layer-by-layer assembled energy gradient of colloidal quantum dots and studied the Förster-type exciton transfer dynamics of both QW and NQD emissions. Our hybrid model system achieved an exciton transfer efficiency of 83.3% at room temperature. The energy gradient with the green- and red-emitting NQDs provided an increased level of exciton transfer efficiency, with an enhancement of 64.2% compared to the bilayer of red-emitting NQDs. Substantially, enhancing the exciton transfer from QW to NQDs, the energy gradient in

QW/NQD/NQD opens up possibilities for optical near field devices. Mastering excitonic pathways in such cascaded systems enables exciting opportunities for future high-efficiency excitonic devices.

This work is supported in part by EU-N4E NoE and TUBITAK under the Project Nos. 109E002, 109E004, 110E010, and 111E217, and in part by NRF-RF-2009-09 and NRF-CRP-6-2010-2. Also, H.V.D. acknowledges additional support from the Turkish Academy of Sciences Distinguished Young Scientist Award (TUBA GEBIP) and European Science Foundation (ESF) European Young Investigator Award (EURYI) Programs and EM acknowledges TUBITAK BIDEB.

¹D. M. Basko, V. M. Agranovich, F. Bassani, and G. C. La Rocca, *Eur. Phys. J. B* **13**, 653–659 (2000).

²M. Achermann, M. A. Petruska, S. Kos, D. L. Smith, D. D. Koleske, and V. I. Klimov, *Nature (London)* **429**, 642 (2004).

³M. Achermann, M. A. Petruska, D. D. Koleske, M. H. Crawford, and V. I. Klimov, *Nano Lett.* **6**, 1396 (2006).

⁴S. Nizamoglu, E. Sari, J.-H. Baek, I.-H. Lee, and H. V. Demir, *New J. Phys.* **10**, 123001 (2008).

⁵T. Franzl, T. A. Klar, S. Schietinger, A. L. Rogach, and J. Feldmann, *Nano Lett.* **4**, 1599 (2004).

⁶T. A. Klar, T. Franzl, A. L. Rogach, and J. Feldmann, *Adv. Mater.* **17**, 769 (2005).

⁷N. Cicek, S. Nizamoglu, T. Ozel, E. Mutlugun, D. U. Karatay, V. Lesnyak, T. Otto, N. Gaponik, A. Eychmueller, and H. V. Demir, *Appl. Phys. Lett.* **94**, 061105 (2009).

⁸N. Gaponik, D. V. Talapin, A. L. Rogach, K. Hoppe, E. V. Shevchenko, A. Kornowski, A. Eychmueller, and H. Weller, *J. Phys. Chem. B* **106**, 7177–7185 (2002).

⁹M. Naruse, E. Rge, K. Kobayashi, and M. Ohtsu, *Phys. Rev. B* **82**, 125417 (2010).

¹⁰See supplementary material at <http://dx.doi.org/10.1063/1.4724109> for more details about theoretical analysis and for the more details about the nutation process.